Journal of Translational Medicine

RESEARCH

Open Access

Sodium tanshinone IIA sulfonate promotes proliferation and differentiation of endogenous neural stem cells to repair rat spinal cord injury via the Notch pathway

Wenqing Zhong[1†], Luchun Xu[1†], Guozheng Jiang[1†], Yushan Gao[2], Jiawei Song[1], Yukun Ma[1], Guanlong Wang[1], Jiaojiao Fan[1], Wenhao Li[1], Shibo Zhou[1], Yongdong Yang[1*] and Xing Yu[1*]

Abstract

Background Interventions that promote the proliferation of endogenous neural stem cells (ENSCs) and induce their differentiation into neurons after spinal cord injury (SCI) hold significant potential for SCI repair. Tanshinone IIA (TIIA) exhibits extensive neuroprotective effects, and its derivative, sodium tanshinone IIA sulfonate (STS), has enhanced water solubility, making it easier to prepare injectable formulations and increasing bioavailability. STS injections have been extensively utilized in the treatment of cardiovascular and cerebrovascular diseases, and their clinical application in SCI shows promising potential. However, it remains unclear whether STS can promote spinal cord injury repair in rats by modulating the proliferation and differentiation of ENSCs, and the underlying regulatory mechanisms are yet to be elucidated.

Methods In this study, an incomplete spinal cord injury model was established in rats using the NYU spinal cord impactor. The regulatory effects of STS on ENSCs in rats post-SCI were observed by detecting the NSC marker Nestin, the neuronal marker NeuN, and the astrocyte marker GFAP. Additionally, rat behavioral assessments, histopathology, serum inflammation indices, and Notch signaling pathway activation were evaluated. In vitro experiments utilized an lipopolysaccharide (LPS)-induced rats spinal cord NSCs inflammation model. The effects of STS on the proliferation and viability of rats spinal cord NSCs were assessed using the CCK-8 assay and immunofluorescence cell counting. The mechanisms by which STS regulates NSC proliferation and differentiation via the Notch pathway were verified using immunofluorescence, Western blot, and RT-PCR techniques.

Results In vitro, STS significantly reduced the levels of inflammatory indices in the LPS-induced rats NSCs inflammation model and improved the viability of rats NSCs following inflammatory injury. STS also significantly

[†]Wenqing Zhong, Luchun Xu and Guozheng Jiang contributed equally to this work.

*Correspondence:
Yongdong Yang
yyd8817@163.com
Xing Yu
yuxingbucm@163.com

Full list of author information is available at the end of the article

increased the proliferation of NSCs and their differentiation into neurons while reducing their differentiation into astrocytes. Moreover, LPS significantly activated the Notch pathway, similar to the effects of the Notch pathway agonist valproic acid (VPA), whereas STS intervention could inhibit the LPS- or VPA-induced activation of the Notch pathway. In vivo, STS markedly improved the hindlimb motor function of rats with SCI, decreased the levels of pro-inflammatory factors IL-6 and TNF-α, and increased the level of the anti-inflammatory factor IL-10, thereby improving the pathological morphology of the injured spinal cord in rats post-SCI. STS effectively promoted the proliferation of ENSCs post-SCI, facilitated their differentiation into neurons, and inhibited their differentiation into astrocytes. Additionally, STS suppressed the excessive activation of the Notch signaling pathway following SCI.

Conclusion STS promotes the proliferation of ENSCs post-SCI in rats, induces their differentiation into neurons, and inhibits their differentiation into astrocytes, thereby improving the pathological morphology of the injured spinal cord and promoting the recovery of hindlimb motor function in rats post-SCI. Furthermore, the regulatory effects of STS on the proliferation and differentiation of ENSCs post-SCI in rats may be related to its inhibition of the excessive activation of the Notch signaling pathway.

Keywords Sodium tanshinone IIA sulfonate, Spinal cord injury, Endogenous neural stem cells, Proliferation, Differentiation, Notch signaling pathway

Introduction

Spinal cord injury (SCI) is a severe neurological disorder that can lead to a range of sensory and motor impairments [1, 2]. With the increasing incidence of SCI worldwide, it has become a major burden on society, patients, and caregivers [3, 4]. The complex pathophysiological mechanisms of SCI involve primary injury due to the initial mechanical trauma and secondary injury caused by factors such as inflammation, oxidative stress, autophagy, and apoptosis. Current treatments can only alleviate symptoms and reduce complications, but no definitive cure exists [5, 6]. Recent studies have found that endogenous neural stem cells (ENSCs) can proliferate and differentiate into neurons and astrocytes after SCI [7, 8]. However, the complex microenvironment post-injury limits the proliferation of ENSCs and results in a lower differentiation rate into neurons and a higher rate into astrocytes, thereby limiting functional recovery of the spinal cord [9, 10]. Therefore, developing regenerative strategies that promote the proliferation and neuronal differentiation of ENSCs holds significant potential.

Tanshinone IIA (TIIA) is an important lipophilic active component of the traditional Chinese herb Danshen (*Salvia miltiorrhiza* Bge.). Pharmacological studies have confirmed that TIIA has extensive neuroprotective effects in various CNS diseases, including anti-inflammatory, immune-regulating, and antioxidant activities [11, 12]. Sodium tanshinone IIA sulfonate (STS), a derivative of TIIA, significantly enhances water solubility, making it easier to prepare injectable formulations and increasing bioavailability [13, 14]. Previous studies have shown that STS can improve motor and sensory functions in rats with SCI, repair damaged blood-spinal cord barrier structures, modulate microglial phenotypic polarization, and reduce inflammatory responses, thus exerting neuroprotective effects [15, 16]. Additionally, our previous research found that STS can promote the remodeling of spinal neural pathways controlling the lower urinary tract, thereby improving neurogenic lower urinary tract dysfunction caused by SCI [17]. However, the effects of STS on the proliferation and differentiation of neural stem cells (NSCs) after SCI remain unclear and require further exploration.

Based on this, we designed both in vivo and in vitro experiments to determine whether STS can regulate the proliferation and differentiation of ENSCs post-SCI and to preliminarily elucidate its mechanism of action. Our results indicate that STS can promote the proliferation of rats ENSCs, induce their differentiation into neurons, and inhibit their differentiation into astrocytes. Furthermore, the regulatory effects of STS on NSCs may be achieved by inhibiting the excessive activation of the Notch signaling pathway post-SCI. This finding provides new insights into the treatment of SCI and offers more options and directions for future research.

Methods

Fabrication of animal models and drug delivery methods

A total of 108 female adult Sprague–Dawley (SD) rats weighing 280–320 g were used in this study. The rats were purchased from SPF (Beijing) Biotechnology Co., Ltd. The Animal Ethics Committee of Beijing University of Chinese Medicine approved all experimental and animal procedures outlined in this study (Approval Number: BUCM – 2023052602–2135, Beijing, China), conducted in accordance with the principles described in the National Institutes of Health (NIH) Guide for the Care and Use of Laboratory Animals (NIH Publications No. 8023). The rats were housed in a controlled environment with a 12:12 h light-dark cycle and had unrestricted access to food and water. Each rat was assigned a numbered ear tag. The rats were randomly divided into three

groups: sham group ($n = 36$), SCI group ($n = 36$), STS group ($n = 36$). The rats were anesthetized with 4% pentobarbital (0.1 mL/100 g, intraperitoneal injection). Subsequently, a laminectomy was performed at the T9 segment to expose the spinal cord. An incomplete SCI animal model (height: 25 mm, weight: 10 g) was established using an NYU impactor (model-II manual, NYU, USA). The sham group underwent laminectomy without SCI. The STS group was administered daily intraperitoneal injections of STS solution (provided by SPH No.1 Biochemical & Pharmaceutical Co., Ltd.; Shanghai, China) at a dose of 20 mg/kg for 14 consecutive days, based on our previous research results [17]. The sham and SCI groups received equal amounts of saline intraperitoneally for 14 consecutive days. All three groups were immediately administered intraperitoneal injections of EDU (5 mg/kg) (Cat# ST067, Beyotime Biotechnology, Shanghai, China) twice daily for 14 days, followed by injections every three days until the day of sampling, with one final injection four hours before sampling. EDU intraperitoneal injection labels proliferating cell nuclei after SCI, providing greater accuracy and ease of use compared to the previously used BrdU.

Behavioral evaluations

Basso, Beattie, Bresnahan locomotor rating scale

The Basso, Beattie, and Bresnahan (BBB) locomotor rating scale was used to assess hind limb motor function [18]. The scale evaluates stepping ability, bilateral joint movement, coordination, and trunk stability, with higher scores indicating better motor function. Assessments were conducted before injury and at 1, 3, 7, 14, 21, 28, and 56 days post-injury in an open field.

Inclined plate test

According to previous reports [19], a rough-surfaced rectangular wooden board was prepared. Rats were positioned on the board with their heads against the wall, and the longitudinal axis of their bodies parallel to the long side of the board. The board was then raised against the wall, and the angle formed between the long side of the board and the experimental operating table was measured with a goniometer. The result was recorded as the maximum angle at which the rat could stay on the inclined board for at least 5 s. Assessments were performed before injury and at 1, 3, 7, 14, 21, 28, and 56 days post-injury.

Tissue processing

At designated time points post-injury, rats were anesthetized with 4% pentobarbital and intracardially perfused with at least 200 mL of phosphate-buffered saline (PBS), followed by 400 mL of 4% paraformaldehyde (Cat# P0099, Beyotime Biotechnology). Subsequently, 1.5 cm segments were obtained from the injured lesion. The remaining rats were sacrificed without perfusion, and the spinal cord was extracted for further analysis. Tissues were stored at − 80 ℃. The spinal cord tissue from perfused rats was used for tissue sectioning and staining, while the spinal cord tissue from non-perfused rats was used for molecular biology experiments.

Paraffin section preparation

At designated time points after injury, the tissue around the injury site (about 1.5 cm) was obtained and fixed in paraformaldehyde for at least 48 h. Subsequently, the tissue was dehydrated in a gradient series of alcohol, and followed cleared by xylene, embedded in paraffin, cut into 5 μm serial sections, heated at 37 ℃ for at least 4 h, and then stored at room temperature.

Serum preparation

At 14 days post-SCI, blood (5 mL) was collected from the abdominal aorta of normal or injured rats in each group. After standing for about 1 h, the blood was centrifuged at 4 ℃, 3000 rpm, for 15 min. The supernatant serum was collected into 1 mL sterile centrifuge tubes. To maximize the use of the rats, fresh spinal cord tissue was immediately collected on ice for subsequent analysis.

Histological staining

Hematoxylin and eosin (HE) and Nissl staining were performed at 14 and 56 days post-SCI. For HE staining, the prepared spinal cord tissue sections were de-paraffinized, stained with hematoxylin (for 30 s) and eosin (for 30 s), dehydrated, and sealed for microscopic examination. For Nissl staining, spinal cord tissue sections were de-paraffinized and washed with distilled water. According to the steps described in the Nissl staining kit (Cat# G1430, Solarbio Life Science, Beijing, China), the sections were immersed in tar violet staining solution, stained at 56 ℃ for 60 min, rinsed with distilled water for 30 s, differentiated in Nissl differentiation solution for 30 s to 2 min, and observed under a light microscope until satisfactory staining was achieved. After dehydration, sections were treated with xylene until transparent and fixed with neutral resin for further microscopic examination.

Tissue Immunofluorescence staining

The prepared spinal cord tissue sections were de-paraffinized and placed in a repair box filled with ethylenediaminetetraacetic acid (EDTA) disodium salt (pH 8.0) antigen repair solution and subjected to antigen repair in a microwave oven. After natural cooling, the slides were placed in PBS and washed 3 times. The sections added bovine serum albumin (BSA) dropwise and closed for 10 min. Primary antibodies namely Nestin (1:100, Cat# 19483-1-AP, ptg inc., Wuhan, China), NeuN (1:200, Cat#

DF6145, Affinity Biosciences, Zhangjiagang, China), GFAP (1:200, Cat# GB12090100, Servicebio, Wuhan, China) were then incubated with the sections overnight at 37 °C. Subsequently, secondary antibodies, namely goat anti-mouse IgG (1:200, Cat# ab150117, Abcam plc.) and goat anti-rabbit IgG (1:200, Cat# ab6717, Abcam plc.) were incubated with the sections in a humidified and light-protected chamber for 1 h. After washing, the sections were stained with 4',6-diamidino-2-phenylindole (DAPI, Cat# ab104139, Abcam plc.) sealing agent. Digital slide scanner was used to capture images, and semi-quantitative analysis of the expression of Nestin, NeuN and GFAP was performed. The count of positive cells was measured using Image J software (National Institutes of Health).

Culture and identification of NSCs

Primary rat spinal cord NSCs (Cat# CP-R313, Boster Biological Technology, Ltd., Wuhan, China) were extracted from fetal rat spinal cords and cultured using the associated complete NSC culture medium (Cat# CP-R313, Boster Biological Technology, Ltd.). The medium was changed every 2–3 days, and the cells were passaged after 6 days of culture. Third-generation cells were inoculated into six-well plates for further experiments.

Nestin was used to identify NSCs. Immunofluorescence staining was performed on the suspension and walled cells. Poly-L-lysine-coated coverslips were placed in a 6-well plate, and 1 mL of a third-generation NSC suspension at a density of 1×10^4 cells/mL was added to each well. The cells were cultured in a 37 °C, 5% CO_2 incubator for 24 h, after which the coverslips were removed. The cells were washed three times with PBS buffer, with each wash lasting 5 min. Then, the cells were then fixed with 4% paraformaldehyde for 30 min and washed three times with PBS. Nestin antibody (1:50, Cat# 19483-1-AP, ptg inc.), was then incubated overnight at 4℃, followed by incubation with secondary antibody under low light, namely goat anti-rabbit IgG (1:500, Cat# ab6717, Abcam plc.) at room temperature for 120 min. Finally, the cells were stained with DAPI for 10 min under low light, followed by fluorescence microscopy.

Effects of STS and LPS on NSC viability and proliferation

NSCs were seeded into three 96-well plates at a density of 1 × 10^5 cells/100 μL per well and cultured with primary NSC medium containing various concentrations of LPS (5 μg/mL, 10 μg/mL, 20 μg/mL, 50 μg/mL). A control group without LPS and a blank group with no cells were also set up. At 24, 48, and 72 h, one 96-well plate was taken, and 10 μL of Cell Counting Kit-8 (CCK-8) solution was added to each well and incubated for 1 h. The absorbance at 450 nm was measured using a microplate reader to reflect cell viability and proliferation.

STS was stored in a light-protected manner at -20 °C. After removing from the freezer, the required amount was dissolved in DMSO to prepare a 10 mM stock solution, which was aliquoted and stored at -80 °C. The stock solution was diluted with primary NSC medium to prepare working solutions at concentrations of 1 μM, 3 μM, 5 μM, 10 μM, and 20 μM. At 24, 48, and 72 h, cell viability and proliferation were assessed using the CCK-8 assay.

To explore the effects of STS on LPS-treated NSCs, the cells were divided into the following groups: control group (no STS and no LPS), STS group (10 μg/mL STS for 24 h), LPS group (20 μg/mL LPS for 48 h), and LPS + STS group (20 μg/mL LPS for 48 h followed by 10 μg/mL STS for 24 h). The control group received primary NSC medium, the STS group received medium with 10 μg/mL STS for 24 h, the LPS group received medium with 20 μg/mL LPS for 48 h, and the LPS + STS group received medium with 20 μg/mL LPS for 24 h followed by medium with 10 μg/mL STS for 24 h. Cell viability and proliferation were assessed using the CCK-8 assay and immunofluorescence cell counting.

Differentiation of NSCs

Third-generation NSCs were switched to differentiation medium (99% primary NSC medium + 1% fetal bovine serum) for differentiation culture. The cells were divided into control, STS, LPS, LPS + STS, VPA, and VPA + STS groups. Following Platta's method, the Notch signaling pathway was significantly activated by 4 mM VPA for 48 h [20]. The differentiation culture period was 5 days, with the medium changed 1–2 times.

Cellular Immunofluorescence assay

Poly-L-lysine-coated coverslips were placed in a 24-well plate, and 1 mL of a third-generation NSC suspension at a density of 1×10^4 cells/mL was added to each well. The cells were cultured in a 37 °C, 5% CO_2 incubator for 24 h, after which the coverslips were removed. The cells were washed three times with PBS buffer, with each wash lasting 5 min. Cells were fixed on slides with 4% paraformaldehyde, washed three times with PBS for 2 min each, and incubated with blocking solution at 37 °C for 60 min. Primary antibodies (Nestin, 1:100, Cat# 19483-1-AP, ptg inc.; NeuN, 1:200, Cat# DF6145, Affinity Biosciences; GFAP, 1:200, Cat# GB12090100, Servicebio) were added and incubated overnight at 4 °C. The next day, the secondary antibodies and DAPI were added and incubated under low light. Finally, images were captured using fluorescence microscopy.

Western blot analysis

At designated time points after injury, total protein was extracted from cells or spinal cord tissues. Spinal cord NSCs and tissues were homogenized in ice-cold

RIPA lysis buffer (Cat# R0010, Solarbio Life Sciences). After determining the protein concentration using a BCA assay kit (Cat# 23225, Thermo Fisher Scientific, Waltham, USA), the proteins were detached using 10% sodium dodecyl sulfate–polyacrylamide gel electrophoresis (PAGE). Thereafter, the proteins were transferred to polyvinylidene fluoride (PVDF) membranes, which were blocked with 0.1% TBS-T containing 5% skim milk powder for 1 h. Subsequently, the membrane was incubated overnight at 4 °C with the following primary antibodies: Nestin (1:1000, Cat# 19483-1-AP, ptg inc.), NeuN (1:1000, Cat# DF6145, Affinity Biosciences), GFAP (1:1000, Cat# GB12090100, Servicebio), Notch1 (1:1000, Cat# 4350T, Cell Signaling Technology, Danvers, USA), DLL1 (1:1000, Cat# 2588T, Cell Signaling Technology), Hes5 (1:1000, Cat# ab194111, abcam plc.), β-actin (1:3000, Cat# AF7018, Affinity Biosciences). After incubation, the membrane was washed and secondary antibodies were added and incubated at 37 °C for 60 min. After which, the membrane was washed again, and immersed in enhanced chemiluminescence (ECL) color development solution for 4 min, followed by exposure, imaging, and fixing in a darkroom. Finally, ImageJ software (National Institutes of Health) was used to quantify the protein expression in each band.

Real-time polymerase chain reaction (RT-PCR)

Total RNA was extracted from the injured spinal cord and spinal cord NSCs using TRIzol reagent (Invitrogen, USA). The extracted RNA (1 μg) was reverse transcribed into cDNA using the SuperScript III RT kit (invitrogen, USA). Real-time Polymerase Chain Reaction (RT-PCR) was performed using a Real-Time PCR kit (invitrogen, USA). The reaction system consisted of 2 μl of cDNA, 10 μl of SYBR mix, and 1 μl of each primer. The PCR conditions were as follows: preincubation at 95℃ for 5 min, followed by 40 cycles of denaturation at 94 ℃ for 10 s, annealing at 58 ℃ for 20 s and extension at 72 ℃ for 20 s using the RT-PCR machine (Applied Biosystems, Carlsbad, CA, USA). The primer details are provided in Table 1 (Nestin, NeuN, GFAP, Notch1, DLL1, Hes5 and β-actin).

Table 1 Primers of RT-PCR used in this study

Target	Forward (5′-3′)	Reverse (5′-3′)
Nestin	GACCTCCTTAGCCACAACCC	GTTCCCAGATTTGCCCCTCA
NeuN	CCCCCATTCCAACTTACGGA	AACGGACAAGAGAGTGGTGG
GFAP	GGGCGAAGAAAACCGCATC	TGGGCACACCTCACATCAC
Notch1	CACCCGCCAGGAAAGAGG	CAGCGTTAGGCAGAGCAAGG
DLL1	TATCACACCTGGAGCCGAGA	AGGGATGCCCGGAAAGTCTA
Hes5	ATGCTCAGTCCCAAGGAGAAA	CGAAGGCTTTGCTGTGCTTC
β-actin	CTGAACGTGAAATTGTCCGAGA	TTGCCAATGGTGATGACCTG

Enzyme-linked immunosorbent assay (ELISA)

ELISA kits were used to investigate the expression levels of tumor necrosis factor (TNF)-α, interleukin (IL)-10, and IL-6 in rat serum according to the manufacturer's instructions (all ELISA kits were purchased from Jianglai Bio, Shanghai, China). For spinal cord NSC, a small amount of culture medium was collected and centrifuged at 1200 rpm for 5 min to obtain the cell supernatant. The levels of TNF-α and IL-6 in the supernatant were then detected using ELISA kits. Absorbance was measured at 450 nm using a microplate reader (Multiskan MS 352, Labsystems, Finland), and the concentrations of TNF-α, IL-10, and IL-6 were calculated from standard curves.

Statistical analysis

Statistical analysis and data visualization were performed using SPSS 26.0 software (IBM Corp., Armonk, NY, USA) and GraphPad Prism 8.0 software (GraphPad software Inc., San Diego, CA, USA). Continuous variables were expressed as means ± S.D. The normality and homogeneity of variance were checked to ensure that the data followed a normal distribution and showed homogeneity of variance. Subsequently, one-way analysis of variance (ANOVA) was used for multiple comparisons. For continuous data that did not meet the normal distribution criteria, non-parametric tests were used. A significance level of $P < 0.05$ was considered statistically significant.

Results

STS treatment promotes Attenuation of LPS-induced inflammation and proliferation in NSCs

Initially, the third generation NSCs were identified using the marker Nestin through immunofluorescence staining (Fig. 1A). NSCs from the third generation were used for subsequent experiments. Cell viability of spinal cord NSCs was assessed using CCK8, demonstrating a time and concentration-dependent toxicity of LPS. Based on these results, 20 μg/mL of LPS intervention for 48 h was chosen as the optimal dose for subsequent experiments due to its significant impact on cell viability (Fig. 1B). Similarly, 10 μM STS intervention for 24 h showed the highest cell viability (Fig. 1C). Therefore, 10 μM STS and 20 μg/mL LPS were selected as the experimental doses. The results showed that STS treatment significantly enhanced cell viability compared to other groups ($P < 0.05$). Additionally, the LPS + STS group exhibited higher cell viability compared to the LPS group ($P < 0.05$) (Fig. 1D). Moreover, the levels of TNF-α and IL-6 were significantly higher in the LPS group compared to other groups ($P < 0.001$), indicating that STS effectively inhibited LPS-induced inflammatory responses (Fig. 1E and F).The immunofluorescence cell counting analysis across four experimental groups, with differential fold changes compared relative to the control group, demonstrated

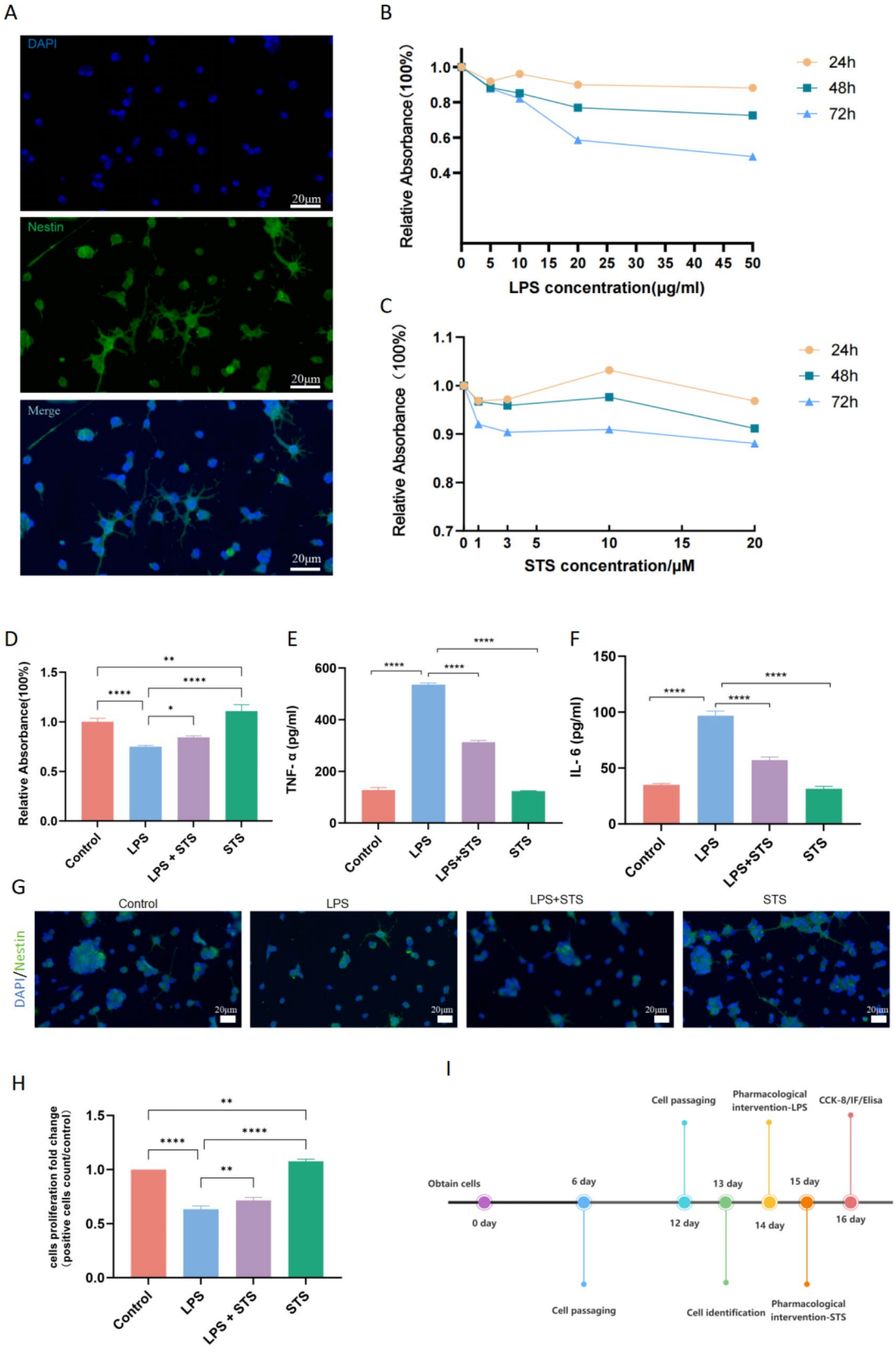

Fig. 1 (See legend on next page.)

(See figure on previous page.)

Fig. 1 STS promotes LPS-induced proliferation of spinal cord neural stem cells. (**A**) Nestin immunofluorescence identification. All DAPI-positive cells are Nestin-positive. DAPI (blue), Nestin(green). Scale bar: 20 μm. (**B**) Changes in spinal cord NSCs relative absorbance with different concentrations and durations of LPS intervention. (**C**) Changes in spinal cord NSCs relative absorbance with different concentrations and durations of STS intervention. (**D**) Effects of STS on LPS-induced relative absorbance of spinal cord NSCs. Data are expressed as the means ± S.D. * represents $P < 0.05$, ** represents $P < 0.01$, **** represents $P < 0.0001$. (**E-F**) ELISA detection of pro-inflammatory factors (IL-6 and TNF-α) levels in spinal cord NSCs. Data are expressed as the means ± S.D. **** represents $P < 0.0001$. (**G**) The effect of STS on LPS-induced Nestin immunofluorescence in spinal cord neural stem cells. (**H**) Comparison of NSCs positive cell counts among different groups.Data are expressed as the means ± S.D. ($n = 4$ per group). ** represents $P < 0.01$, **** represents $P < 0.0001$. (**I**) Timeline of the cell experiment.CCK-8 assays included 6 technical replicates/group across 3 biological repeats, whereas ELISA and IF assays utilized 3 technical and 3 biological replicates per group

that the STS group significantly promoted cell proliferation compared to the other groups ($P < 0.01$) (Fig. 1G and H).

STS treatment alters NSCs differentiation by inhibiting Notch signaling pathway activation

STS treatment was investigated for its effect on NSCs differentiation and its modulation of the Notch signaling pathway activation post-inflammatory injury using immunofluorescence, Western blotting, and RT-PCR. Immunofluorescence staining showed that STS treatment significantly promoted their differentiation towards neurons while reducing differentiation towards astrocytes ($P < 0.05$). Moreover, the effects of STS on NSCs differentiation were inhibited by the Notch pathway agonist VPA ($P < 0.05$) (Fig. 2A-E). Quantitative analysis using Western blotting and RT-PCR confirmed that STS treatment promoted proliferation and differentiation of LPS-induced inflammatory NSCs, consistent with the trends observed in immunofluorescence (Fig. 2F-L). Furthermore, LPS significantly activated the Notch pathway in NSCs, similar to the effect of the Notch pathway agonist VPA, while STS treatment suppressed Notch pathway activation induced by LPS or VPA (Fig. 3A-G). These findings suggest that STS regulates NSCs differentiation by inhibiting activation of the Notch signaling pathway.

STS promotes motor function recovery after SCI

Motor function recovery following SCI was evaluated using the BBB scores and inclined plane test. As shown in Fig. 4A, all rats except those in the sham group exhibited severe motor deficits after injury. From day 3 to day 56 post-injury, the BBB scores in the STS group were significantly higher than those in the SCI group ($P < 0.05$). Similarly, the inclined plane test showed a similar trend (Fig. 4B). These results indicate that STS significantly improves hindlimb motor function in rats after SCI.

STS attenuates inflammatory response after SCI

ELISA was used to measure the levels of inflammatory cytokines in rat serum after SCI. The results showed a significant increase in pro-inflammatory cytokines (IL-6 and TNF-α) levels after SCI. STS treatment effectively reversed this condition and increased the expression of the anti-inflammatory cytokine IL-10 ($P < 0.05$) (Fig. 4C-E). This suggests that STS can effectively inhibit the inflammatory response after SCI.

STS improves pathological morphology of injured spinal cord

Histological staining with HE showed that at 2 weeks and 8 weeks post-injury, the spinal cord tissue in the sham group appeared normal without dead cells or inflammatory infiltration (Fig. 5A and D). The SCI group showed extensive cell debris, loose and disordered structure, inflammatory cell infiltration, and large cavities at the injury center at 2 weeks post-injury (Fig. 5B). In the STS group, some cell debris and inflammatory infiltration were observed at the injury center. The spinal cord tissue showed relatively preserved morphological structure, with cavities of varying sizes present at both the injury center and its margins. (Fig. 5C). At 8 weeks post-injury, the SCI group still showed large cavities at the injury center and scattered cavities of various sizes at the injury edge (Fig. 5E). In the STS group, circular cavities of varying sizes were observed at both the injury center and its margins. A dense accumulation of glial cells was present at the center, with no large cavities observed. (Fig. 5F).

Nissl staining showed that at 2 weeks and 8 weeks post-injury, the sham group exhibited normal morphology of spinal cord neurons, with clear neuronal nuclei and Nissl bodies (Fig. 6A, D). The SCI group at 2 weeks post-injury showed extensive neuronal death, and scattered cell debris and cavities due to secondary injury (Fig. 6B). In the STS group at 2 weeks post-injury, there were some remnants of damaged neurons and cavities (Fig. 6C). At 8 weeks post-injury, the SCI group still showed some normal neurons at the distant injury site, along with some damaged neurons (Fig. 6E). In the STS group, scattered damaged neurons and a widespread distribution of normal neurons were observed (Fig. 6F).

Time and spatial changes of ENSCs after SCI

The time and spatial changes of ENSCs after SCI were studied using immunofluorescence staining. In the sham group, NSCs were primarily distributed in the central canal and gray matter of the spinal cord at all time points (Fig. 7A-C). Fibrous astrocytes (long protrusions, fewer branches, abundant glial filaments in the cytoplasm) were mainly distributed in the white matter, while

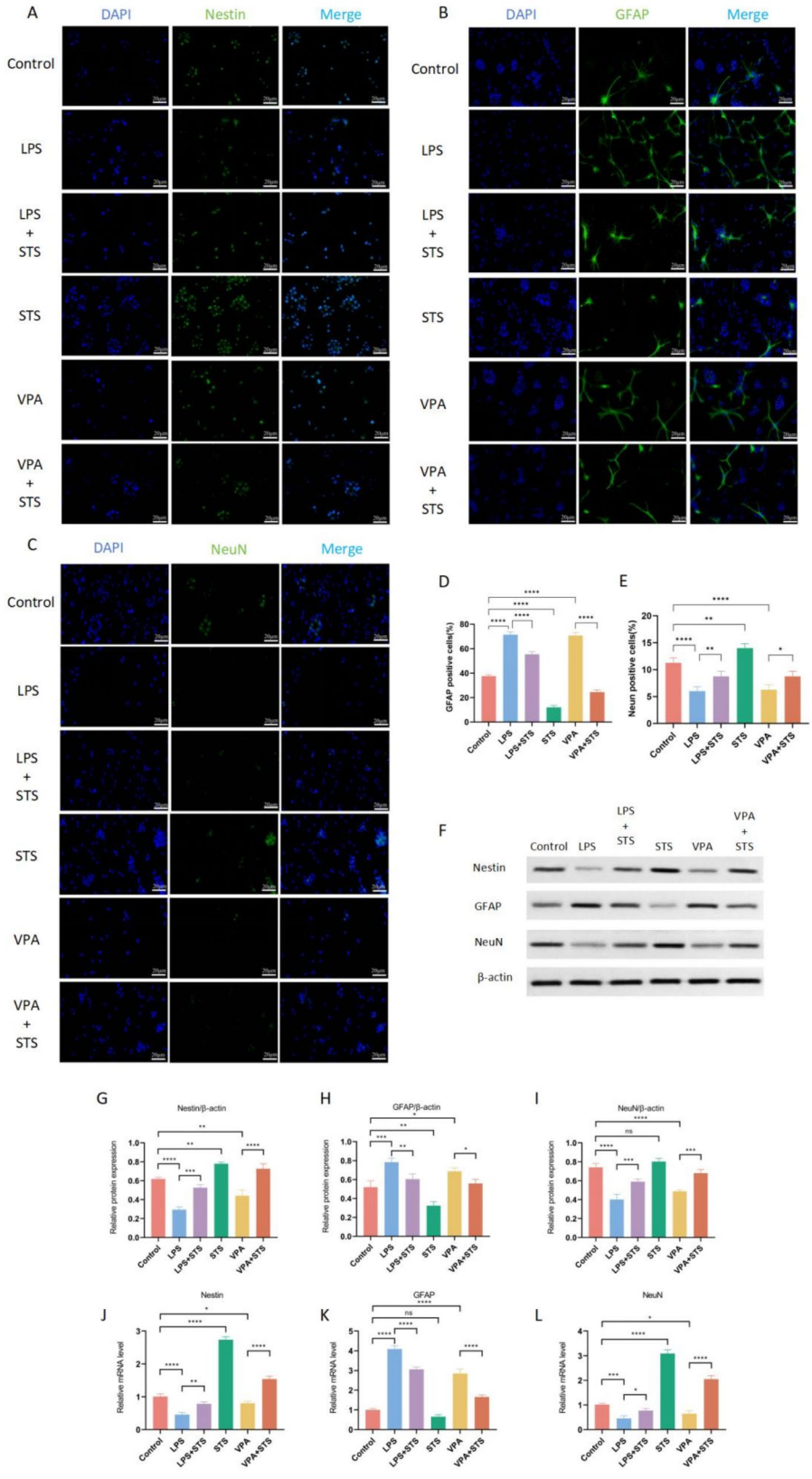

Fig. 2 (See legend on next page.)

(See figure on previous page.)

Fig. 2 STS modulates the differentiation of spinal cord NSCs. (**A-C**) Immunofluorescence staining results for Nestin, GFAP, and NeuN. DAPI (blue), Nestin/GFAP/NeuN (green). Scale bar: 20 μm. (**D-E**) Comparison of the percentage of positive cells relative to DAPI-positive cells for GFAP and NeuN immunofluorescence staining. Data are expressed as the means ± S.D. ($n = 3$ per group). * represents $P < 0.05$, ** represents $P < 0.01$, **** represents $P < 0.0001$, ns represents $P > 0.05$. (**F**) Western blot analysis of Nestin, GFAP, and NeuN. (**G-I**) Quantitative assessment of Nestin, GFAP, and NeuN proteins. Data are expressed as the means ± S.D. ($n = 3$ per group). * represents $P < 0.05$, ** represents $P < 0.01$, *** represents $P < 0.001$, **** represents $P < 0.0001$, ns represents $P > 0.05$. (**J-L**) Quantitative analysis of Nestin, GFAP, and NeuN mRNA levels. Data are expressed as the means ± S.D. ($n = 3$ per group). * represents $P < 0.05$, ** represents $P < 0.01$, *** represents $P < 0.001$, **** represents $P < 0.0001$, ns represents $P > 0.05$

protoplasmic astrocytes (short thick protrusions, more branches, fewer glial filaments in the cytoplasm) were mainly distributed in the gray matter (Fig. 7A-C). Neurons were sparse in the gray matter, with a denser distribution in the anterior horn than in the posterior horn (Fig. 7A-C). In the sham operation group, no proliferating cells were observed. After SCI, there was a significant increase in Edu + cells, indicating proliferation of NSCs (Edu^+ + $Nestin^+$ + $DAPI^+$) primarily in the central canal, injury center, and injury edge (Fig. 7A-C). Reactive astrocytes (enlarged cell bodies and processes) proliferated in response to injury, with a large number observed at 3 days post-injury (Edu^+ + $GFAP^+$ + $DAPI^+$) primarily at the injury edge (Fig. 7A). By day 7 post-injury, astrocyte proliferation decreased, with most located at the injury edge and fewer in the injury center (Fig. 7B). By day 14 post-injury, cavity formation was evident in the injury area, primarily containing astrocytes (Fig. 7C). At 3 days post-injury, the number of proliferating mature neurons (Edu^++ $GFAP^+$+ $DAPI^+$) was low (Fig. 7G). At 7 and 14 days post-injury, the proportion of proliferating mature neurons among proliferating cells increased. Proliferating neurons were primarily located at the injury margin and the dorsal horn of the spinal cord (Fig. 7B-C and G).

At 3 days post-injury, proliferating cells accounted for the highest proportion of total cells, with the SCI group showing a higher percentage than the STS group ($P < 0.05$)(Fig. 7D). At 7 and 14 days post-injury, the proportion of proliferating cells gradually decreased(Fig. 7D). At 3 days post-injury, the majority of proliferating cells in the SCI group were astrocytes, accounting for approximately 30% of total proliferating cells, while in the STS group, the majority of proliferating cells were ENSCs, comprising about 37% of total proliferating cells (Fig. 7E-G). At 7 days post-injury, a significant number of neurons proliferated, with the SCI group showing neurons accounting for 33% of total proliferating cells, and the STS group showing 39%, which was higher than the SCI group ($P < 0.05$) (Fig. 7E-G). At 14 days post-injury, proliferating cells were primarily ENSCs, and the STS group had a higher proportion of proliferating ENSCs and neurons compared to the SCI group ($P < 0.05$), whereas the proportion of proliferating astrocytes was lower in the STS group than in the SCI group ($P < 0.05$) (Fig. 7E-G).

STS promotes proliferation and differentiation of ENSCs after SCI

The effect of STS on proliferation and differentiation of ENSCs after SCI was investigated using immunofluorescence staining, Western blotting, and RT-PCR. Results demonstrated that the proliferation of NSCs was significantly higher in the STS group compared to the SCI group (Figs. 7A-C and E). This indicates that STS further promotes the proliferation of ENSCs after SCI.

Moreover, the arrangement of astrocytes in the STS group was more sparse, with a lower proportion of proliferating cells compared to the SCI group ($P < 0.05$) (Fig. 7A-C and F), suggesting that STS reduces differentiation of ENSCs into astrocytes to some extent after SCI. Additionally, due to direct and secondary injury, more cell debris was observed in the SCI group, whereas STS significantly reduced neuronal cell debris and further promoted differentiation of ENSCs into neurons (Fig. 7A-C and G).

Western blotting and RT-PCR analyses showed similar results, demonstrating that STS intervention effectively upregulated the expression of Nestin and NeuN and downregulated GFAP expression after SCI (Fig. 8). These findings confirm that STS promotes proliferation of ENSCs after SCI while reducing differentiation into astrocytes and promoting differentiation into neurons.

STS May promote proliferation and differentiation of ENSCs after SCI by inhibiting Notch signaling pathway activation

Notch signaling pathway activation may be involved in the regulation of proliferation and differentiation of ENSCs by STS after SCI. Therefore, Western blotting and RT-PCR were used to evaluate the expression of Notch pathway-related proteins and mRNA (Notch1, DLL1, Hes5) in the spinal cord at 3 days, 7 days, and 14 days post-injury. Results showed that at 3 days, 7 days, and 14 days post-SCI, the expression of Notch pathway-related proteins and mRNA (Notch1, DLL1, Hes5) was significantly increased in the SCI group compared to the sham group ($P < 0.05$). However, treatment with STS effectively reversed this upregulation of Notch pathway components (Fig. 9). This suggests that STS can effectively inhibit excessive activation of the Notch pathway after SCI, thereby further promoting proliferation and differentiation of ENSCs.

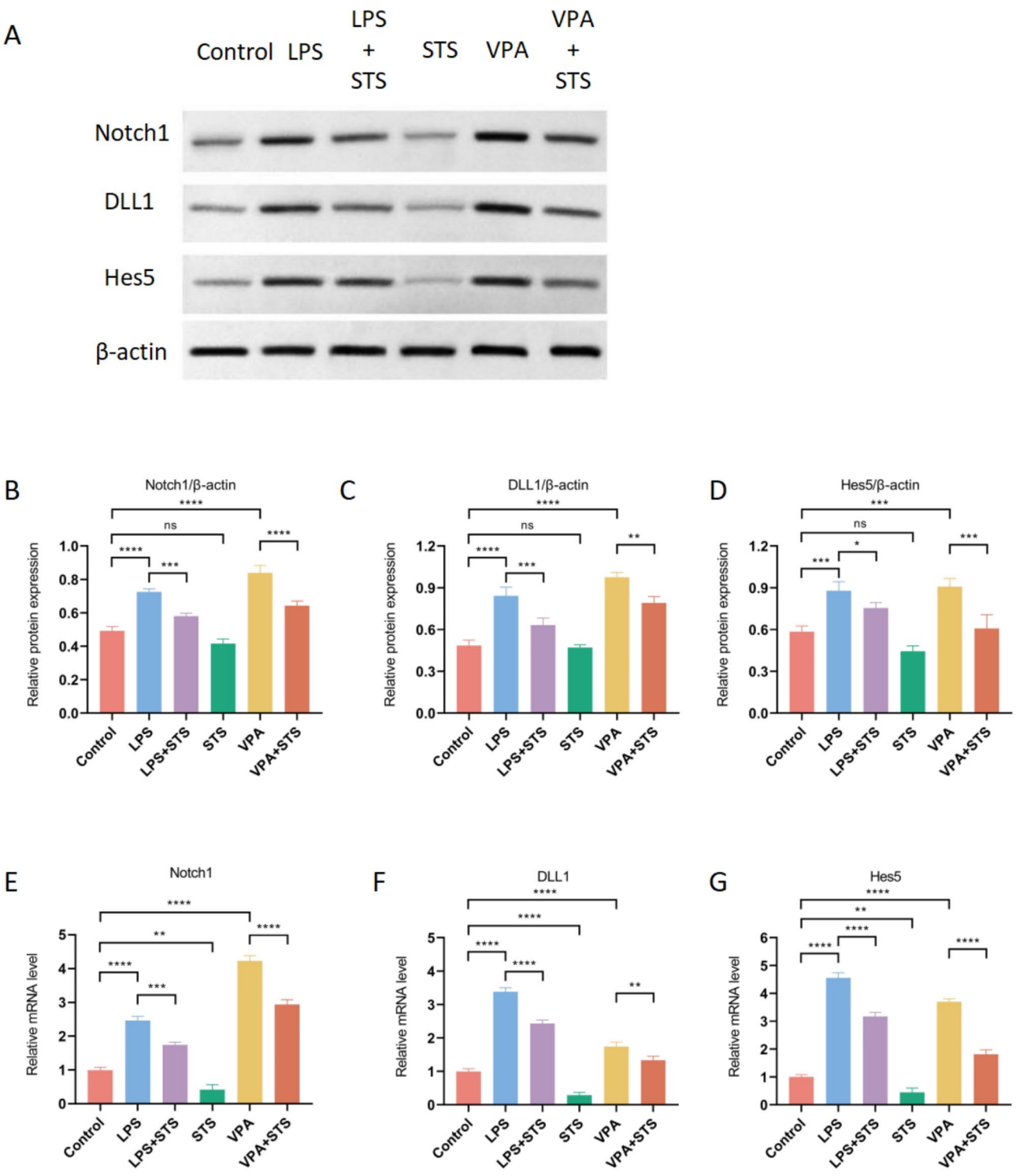

Fig. 3 STS treatment alters NSC differentiation through the Notch signaling pathway. (**A**) Western blot analysis of the Notch signaling pathway (Notch1, DLL1, and Hes5). (**B-D**) Quantitative assessment of Notch signaling pathway proteins (Notch1, DLL1, and Hes5). Data are expressed as the means ± S.D. ($n = 3$ per group). * represents $P < 0.05$, ** represents $P < 0.01$, *** represents $P < 0.001$, **** represents $P < 0.0001$, ns represents $P > 0.05$. (E-G) Quantitative analysis of Notch1, DLL1, and Hes5 mRNA levels. Data are expressed as the means ± S.D. ($n = 3$ per group). ** represents $P < 0.01$, *** represents $P < 0.001$, **** represents $P < 0.0001$

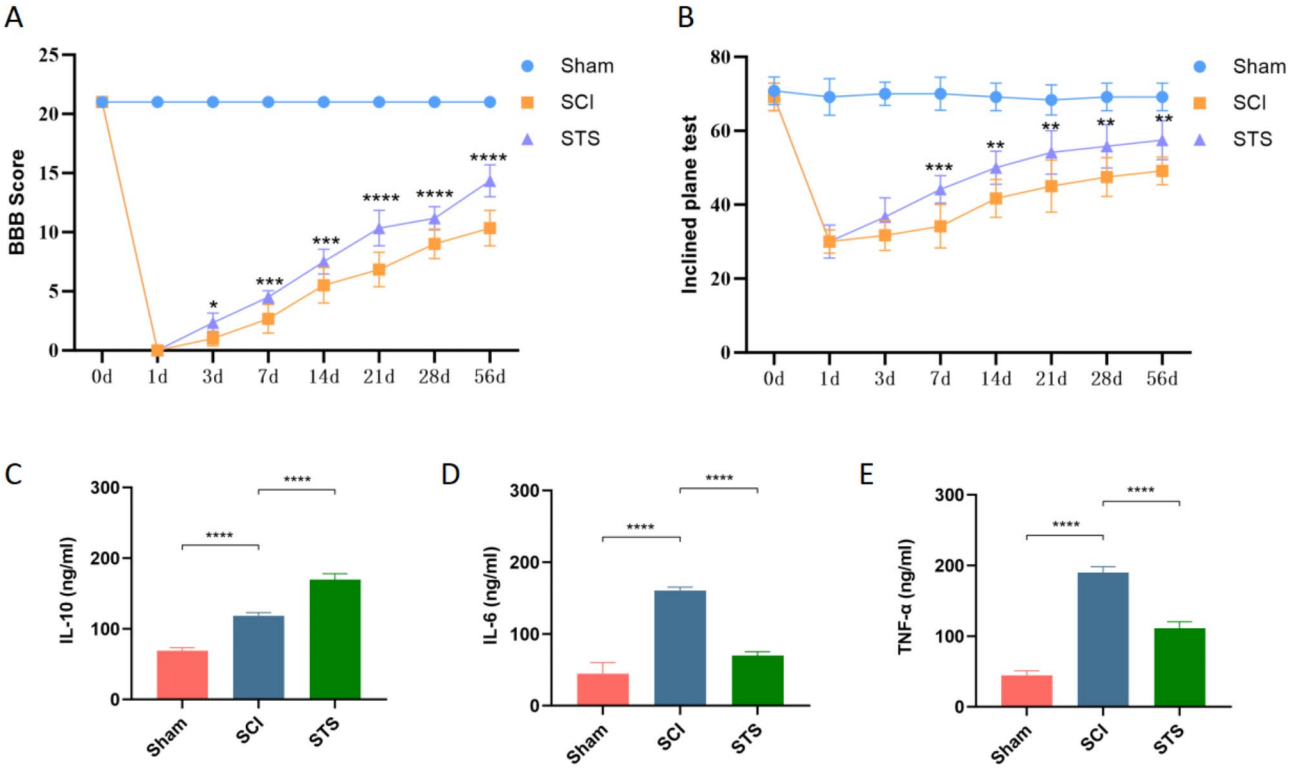

Fig. 4 STS enhances locomotor recovery and lowers pro-inflammatory factors in spinal cord-injured rats. (**A**) BBB scores. (**B**) Inclined plate test. Data are presented as means ± S.D. ($n = 6$ per group). * represents $P < 0.05$, ** represents $P < 0.01$, *** represents $P < 0.001$, **** represents $P < 0.0001$. (**C**) ELISA detection of levels of anti-inflammatory factors (IL-10) and pro-inflammatory factors (IL-6 and TNF-α) in serum of rats with SCI. Data are expressed as the means ± S.D. ($n = 3$ per group). **** represents $P < 0.0001$

Discussion

SCI remains a challenging area of research both in basic and clinical settings, drawing attention from multidisciplinary researchers. Recent advancements in cell transplantation, pharmacological treatments, and tissue engineering have shown progress in SCI repair, with cell transplantation being particularly notable [21–23]. Various exogenous stem cells have been explored for SCI treatment, but issues such as ethical concerns, immune rejection, tumorigenicity, and heterogeneous therapeutic outcomes have hindered their clinical translation [24, 25]. ENSCs, possessing differentiation potential within the body, have emerged as a promising alternative for cell transplantation [26, 27]. ENSCs can proliferate and differentiate into neurons and astrocytes post-SCI, contributing to the partial restoration of damaged neural networks [28]. However, the limited number of ENSCs and their insufficient proliferation and differentiation into neurons pose challenges for substantial neural repair and functional improvement post-SCI [29]. Therefore, finding effective interventions to promote ENSCs proliferation and neuronal differentiation holds immense potential for SCI repair.

Following SCI, activated inflammatory responses exacerbate secondary injury, which in turn impairs neural function recovery post-SCI [30, 31]. The LPS-induced inflammatory injury model of spinal cord NSCs used in this study mimics the physiological and pathological processes of SCI, particularly the impact of secondary injury on NSCs proliferation and differentiation. Thus, our study established an in vitro model of LPS-induced inflammatory injury in spinal cord NSCs to investigate the effects of STS intervention on NSCs proliferation and differentiation. Initial experiments determined that 20 μg/ml LPS intervention for 48 h provided optimal conditions for modeling. CCK-8 confirmed significant cell damage under these conditions, validating successful model construction. ELISA results demonstrated increased secretion of inflammatory cytokines such as IL-6 and TNF-α under these conditions, further confirming successful model induction of inflammatory injury.

Our study investigated the effects of STS treatment on cell viability and inflammatory cytokine expression in spinal cord NSCs post-inflammatory injury. Results showed that STS significantly enhanced cell viability and reduced levels of inflammatory cytokines (TNF-α and IL-6) compared to the LPS-only group. This indicates that STS mitigated inflammatory responses induced by LPS in spinal cord NSCs, thereby improving cellular viability post-inflammatory injury. Additionally, differentiation

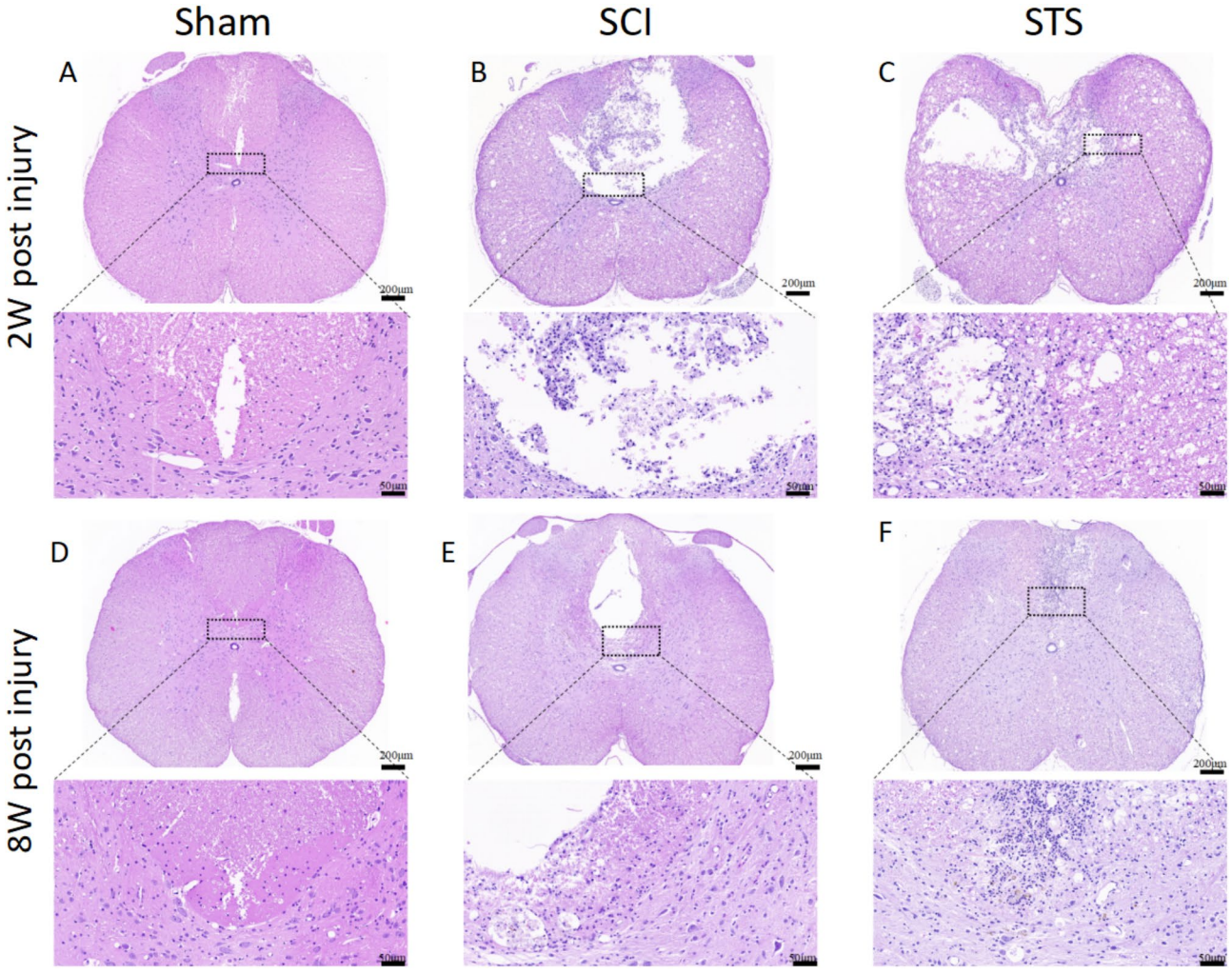

Fig. 5 Spinal cord tissues were collected at 2 and 8 weeks post-injury and embedded in paraffin. Transverse sections were made approximately 1 mm from the center of the SCI. Representative images from each group were randomly selected for HE staining, avoiding the selection of the most severe or the mildest sections. (**A**) Spinal cord at 2 weeks post-injury in the sham group; (**B**) Spinal cord at 2 weeks post-injury in the SCI group; (**C**) Spinal cord at 2 weeks post-injury in the STS group; (**D**) Spinal cord at 8 weeks post-injury in the sham group; (**E**) Spinal cord at 8 weeks post-injury in the SCI group; (**F**) Spinal cord at 8 weeks post-injury in the STS group. Scale bar = 200 μm in spinal cord overall view, and Scale bar = 50 μm in details of the site of injury

cultures of spinal cord NSCs revealed that STS treatment significantly increased NSCs proliferation and their differentiation into neurons while decreasing differentiation into astrocytes. Collectively, these in vitro experimental findings provide a basis for further in vivo research.

To further investigate the effects of STS in vivo, we established an incomplete SCI model in rats using the NYU impactor and treated them with STS via intraperitoneal injection for two weeks post-injury. Results demonstrated that STS effectively improved hind limb motor function in SCI rats, reduced levels of inflammatory cytokines IL-6 and TNF-α, and increased anti-inflammatory cytokine IL-10 levels post-SCI. Histological analysis (HE staining) confirmed that STS reduced cellular debris, inflammatory cell infiltration, and tissue cavitation post-SCI. Nissl staining revealed that STS reduced neuronal death and cavities, facilitating neuronal recovery post-injury. Overall, our in vivo experiments demonstrated that STS improved pathological morphology of the injured spinal cord, attenuated inflammation, and restored hind limb motor function in SCI rats.

Following SCI, ENSCs begin to proliferate, differentiate, and migrate to the injury site in response to primary and secondary injuries [32]. Therefore, we investigated the temporal and spatial changes of ENSCs post-SCI and the effects of STS. Results showed that the peak proliferation of ENSCs occurred at 3 days post-SCI, with a subsequent decline observed from 7 days onwards. At 3 days post-injury, the majority of proliferating cells in the SCI group were astrocytes, while in the STS group, the majority of proliferating cells were ENSCs. At 7 days post-injury, the proportion of proliferating neurons

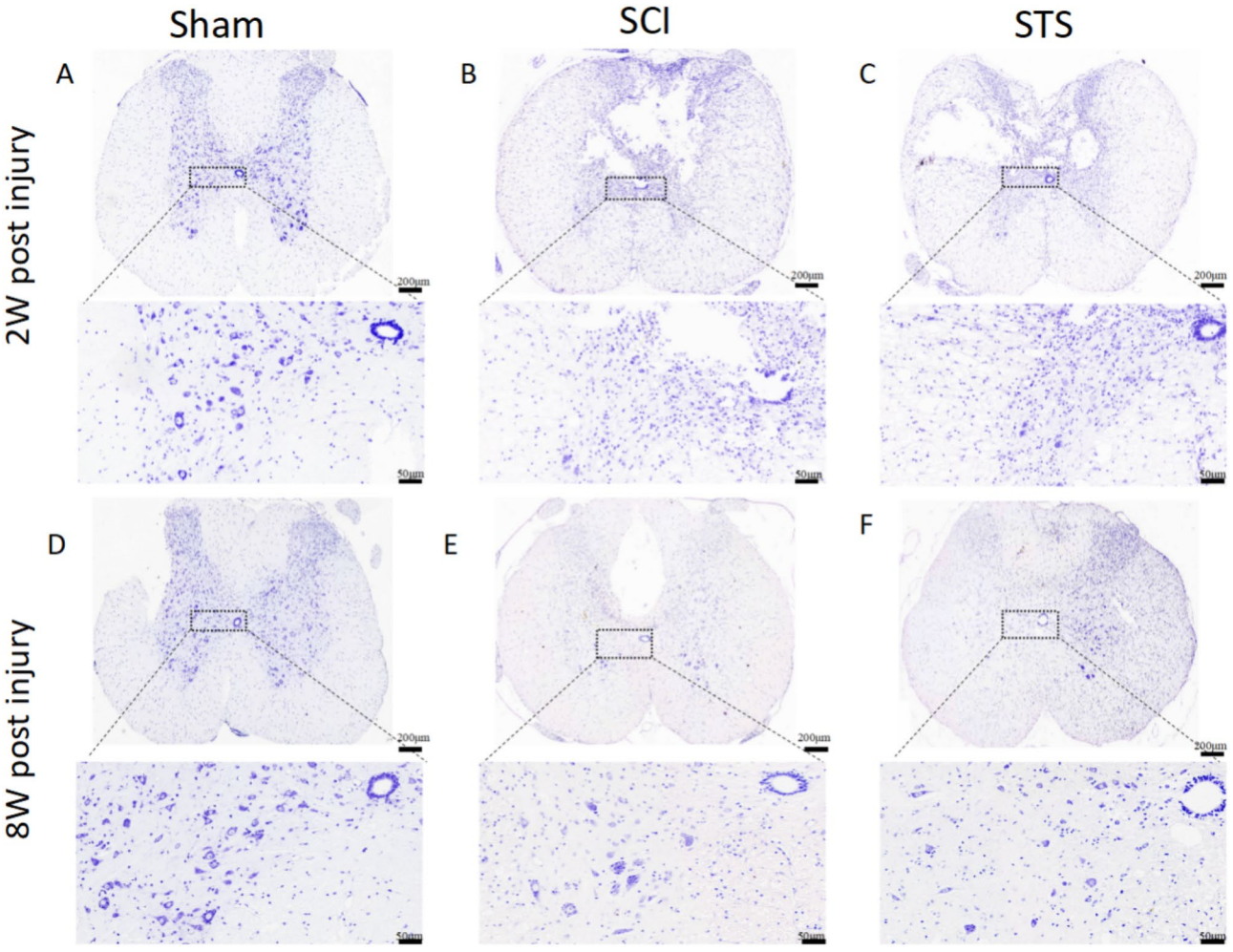

Fig. 6 Nissl staining results of spinal cord tissue at the injury site in rats after SCI. (**A**) Spinal cord at 2 weeks post-injury in the sham group; (**B**) Spinal cord at 2 weeks post-injury in the SCI group; (**C**) Spinal cord at 2 weeks post-injury in the STS group; (**D**) Spinal cord at 8 weeks post-injury in the sham group; (**E**) Spinal cord at 8 weeks post-injury in the SCI group; (**F**) Spinal cord at 8 weeks post-injury in the STS group. Scale bar = 200 μm in spinal cord overall view, and Scale bar = 50 μm in details of the site of injury

increased. At 14 days post-injury, the STS group showed a higher proportion of proliferating ENSCs and neurons compared to the SCI group, while the proportion of proliferating astrocytes was lower in the STS group than in the SCI group. Proliferating NSCs were predominantly distributed in the central canal, injury center, and periphery, while proliferating astrocytes were mainly located at the injury periphery. Proliferating neurons were predominantly located at the injury periphery and dorsal horn of the spinal cord. Spatially, STS-treated groups exhibited increased migration of proliferating NSCs to the injury center and periphery compared to the SCI-only group, where proliferating NSCs were sparsely distributed at the injury periphery. Reactive astrocytes (characterized by enlarged cell bodies and processes) were observed at the injury periphery from 3 days post-SCI onwards, with their density higher in the SCI-only group compared to the STS-treated group at 7 and 14 days post-SCI. Neuronal death due to direct and secondary injuries resulted in fewer neuronal fragments in the STS-treated group compared to the SCI-only group. At 3 days post-injury, mature neuronal proliferation was not evident, while at 7 and 14 days post-injury, STS-treated groups exhibited significantly higher proliferating neurons at the injury periphery compared to the SCI-only group. Thus, STS effectively promoted ENSCs proliferation post-SCI, reduced astrocytic differentiation, and facilitated neuronal differentiation.

Notch signaling pathway inhibits neuronal regeneration and differentiation of NSCs. SCI results in both primary mechanical damage to neurons and secondary damage caused by changes in the injury microenvironment, inflammatory cell infiltration, and elevated levels of inflammatory cytokines [33–35]. Activation of the Notch signaling pathway post-SCI has been shown to inhibit neuronal regeneration and the differentiation of

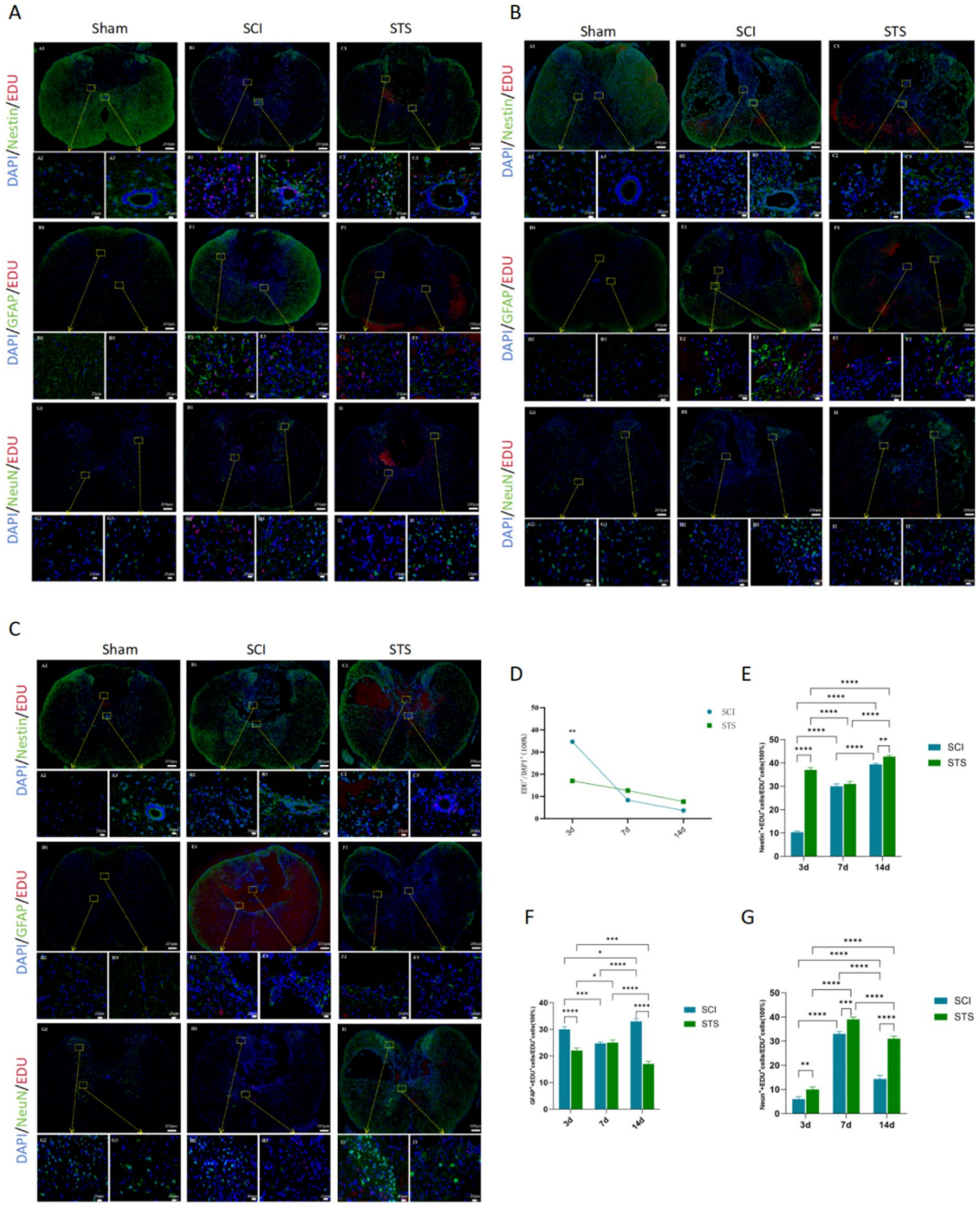

Fig. 7 STS promotes the proliferation of ENSCs and neurons in rats post-SCI. (**A-C**) Immunofluorescence staining of Nestin, GFAP, NeuN, and EDU in spinal cord tissues at 3 d, 7 d, and 14 d post-SCI. DAPI (blue), Nestin/GFAP/NeuN. (green), and EDU (red).Scale bar = 200 μm in the overall view of the spinal cord, and scale bar = 20 μm in detailed views. (**D**) Quantitative comparison of the percentage of EDU-positive cells relative to total cells in the SCI and STS groups at 3 d, 7 d, and 14 d post-SCI. Data are expressed as the means ± S.D. ($n = 3$ per group). ** represents $P < 0.01$. (**E-G**)Quantitative analysis of the percentage of Nestin/EDU, GFAP/EDU, and NeuN/EDU double-positive cells among EDU-positive cells in the SCI and STS groups at 3 d, 7 d, and 14 d post-SCI. Data are expressed as the means ± S.D. ($n = 3$ per group). ($n = 3$ per group).* represents $P < 0.05$, ** represents $P < 0.01$,*** represents $P < 0.001$, **** represents $P < 0.0001$

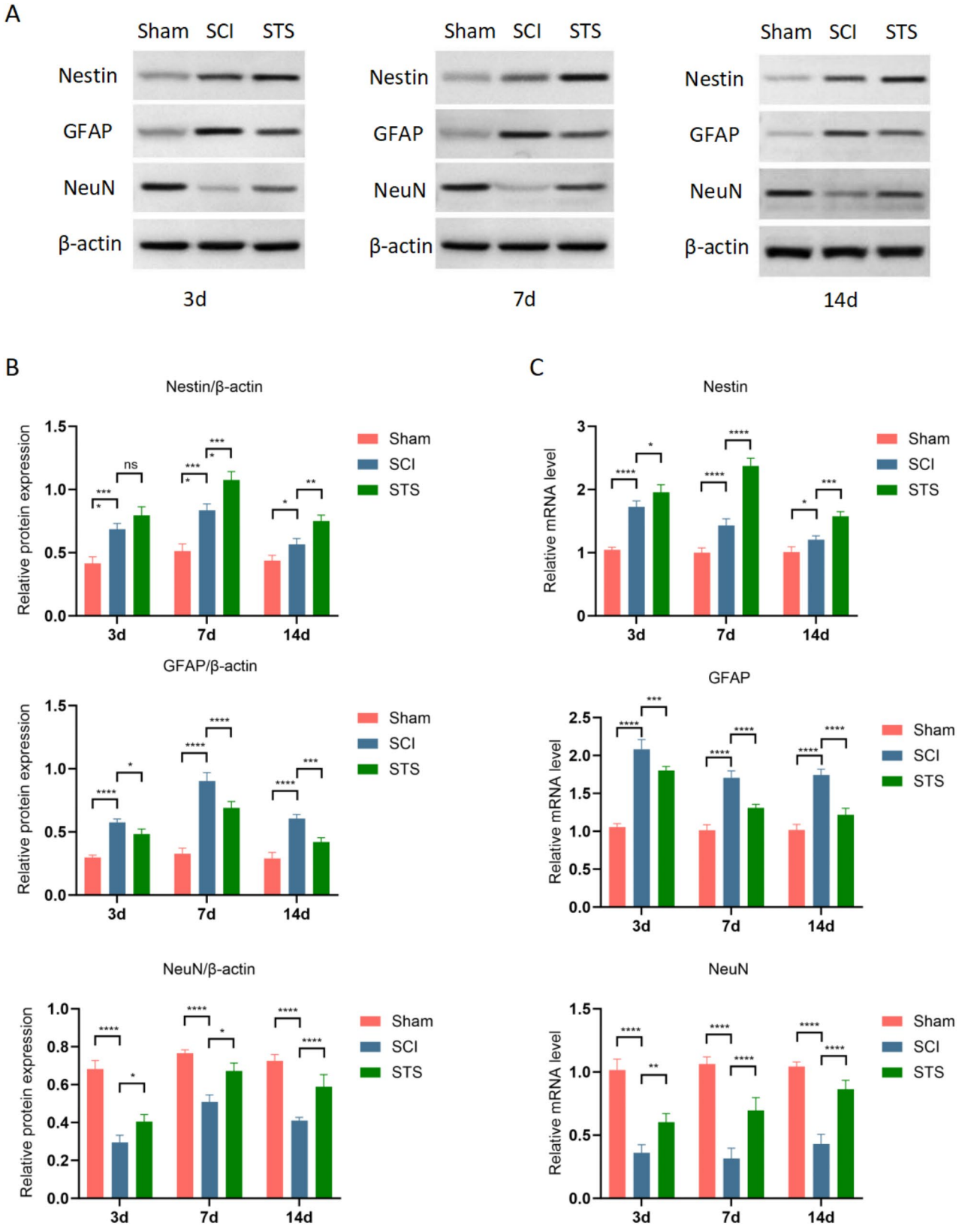

Fig. 8 Expression of NSCs, Astrocytes, and Neurons in Rats After SCI. (**A-B**) Western blot and quantitative analysis of markers for NSCs, astrocytes, and neurons (Nestin, GFAP, and NeuN). Data are expressed as the means ± S.D. ($n = 3$ per group). * represents $P < 0.05$, ** represents $P < 0.01$, *** represents $P < 0.001$, **** represents $P < 0.0001$, ns represents $P > 0.05$. (**C**) Quantitative analysis of Nestin, GFAP, and NeuN mRNA levels. Data are expressed as the means ± S.D. ($n = 3$ per group). * represents $P < 0.05$, ** represents $P < 0.01$, *** represents $P < 0.001$, **** represents $P < 0.0001$

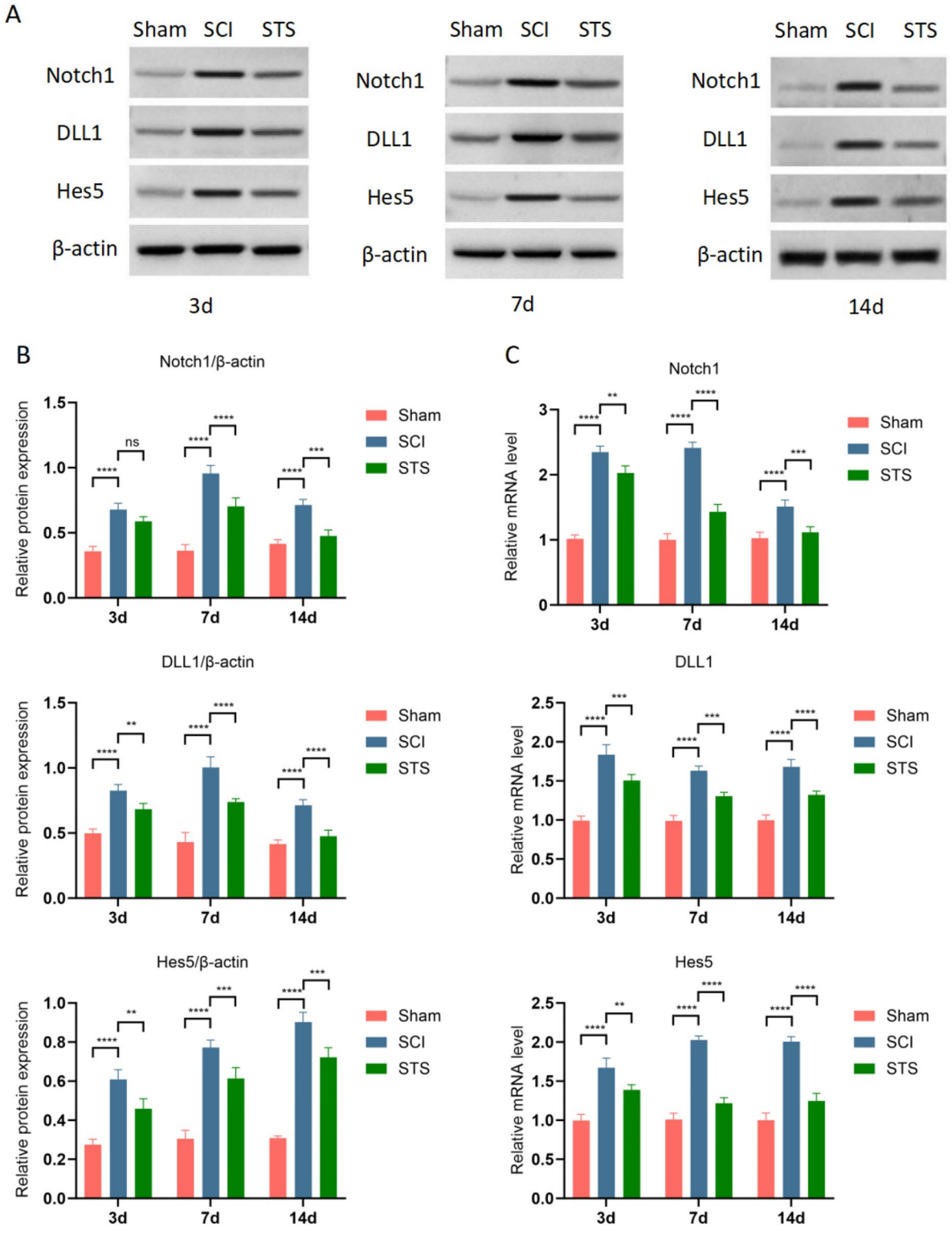

Fig. 9 Potential Mechanism of STS Altering the Proliferation and Differentiation of Endogenous NSCs in Rats After SCI. (**A**) Western blot analysis of the Notch signaling pathway (Notch1, DLL1, and Hes5). (**B**) Quantitative assessment of Notch signaling pathway proteins (Notch1, DLL1, and Hes5). Data are expressed as the means ± S.D. ($n = 3$ per group). ** represents $P < 0.01$, *** represents $P < 0.001$, **** represents $P < 0.0001$, ns represents $P > 0.05$. (**C**) Quantitative analysis of Notch1, DLL1, and Hes5 mRNA levels. Data are expressed as the means ± S.D. ($n = 3$ per group). ** represents $P < 0.01$, *** represents $P < 0.001$, **** represents $P < 0.0001$

NSCs into neurons [36, 37]. Previous studies have highlighted the critical role of the Notch signaling pathway in regulating NSCs proliferation and differentiation [38]. Overexpression of Notch signaling suppresses neuronal regeneration and NSCs proliferation after zebrafish SCI, whereas inhibition of Notch signaling increases neurons and NSCs [39]. NSCs can differentiate into neurons and glial cells, promoting axon regeneration and the construction of neural circuits. They secrete neurotrophic factors via autocrine or paracrine actions to support neuronal survival [40–42]. Activation of the Notch signaling pathway post-SCI plays a crucial role in the proliferation and maintenance of astrocytes, restricting NSCs proliferation and their differentiation into neurons, thereby promoting the differentiation of proliferating NSCs into astrocytes [43, 44]. Astrocytes contribute to the formation of glial scars post-SCI, which act as physical and chemical barriers to axon regeneration, thus hindering spinal cord repair [45].

In our study, we found that LPS significantly activates the Notch pathway in vitro, similar to the Notch agonist VPA. However, STS treatment can inhibit the activation of the Notch pathway induced by LPS or VPA. This suggests that STS regulates NSCs differentiation by suppressing the activation of the Notch signaling pathway. Consistent with our in vitro findings, in rats with SCI at 3, 7, and 14 days post-injury, the expression of Notch pathway-related proteins (Notch1, DLL1, Hes5) and their mRNA levels were significantly elevated in the SCI group compared to the sham-operated group, whereas STS treatment effectively reversed this trend. This indicates that STS effectively inhibits excessive activation of the Notch pathway post-SCI, thereby further promoting ENSCs proliferation and differentiation.

Limitations

It is important to emphasize that our study is limited to rats, and the conclusions cannot yet be generalized to other animals or humans. Although we have explained that the mechanism by which STS promotes NSC proliferation and differentiation into neurons is associated with the inhibition of the Notch signaling pathway's aberrant activation after SCI, the Notch pathway may not act in isolation, and further studies are needed to validate this. Our current research focuses solely on the effects of STS on NSC proliferation and differentiation, while NSC apoptosis also plays a crucial role in neural function repair. More in-depth research is needed to provide a more comprehensive understanding of the impact of STS on NSCs.

Conclusion

STS promotes the proliferation of ENSCs post-SCI in rats, induces their differentiation into neurons, and inhibits their differentiation into astrocytes, thereby improving the pathological morphology of the injured spinal cord and promoting the recovery of hindlimb motor function in rats post-SCI. Furthermore, the regulatory effects of STS on the proliferation and differentiation of ENSCs post-SCI in rats may be related to its inhibition of the excessive activation of the Notch signaling pathway.

Abbreviations

ENSCs	Endogenous neural stem cells
SCI	Spinal cord injury
T IIA	Tanshinone IIA
STS	Sodium Tanshinone IIA sulfonate
LPS	Lipopolysaccharide
VPA	Valproic acid
SD	Sprague-Dawley
BBB	Basso, Beattie and Bresnahan
PBS	Phosphate-buffered saline
HE	Hematoxylin and eosin
BSA	Bovine serum albumin
EDTA	Ethylenediaminetetraacetic acid
RT	PCR-Real-time Polymerase Chain Reaction
Elisa	Enzyme-linked immunosorbent assay
TNF	Tumor necrosis factor

Acknowledgements

Not applicable.

Author contributions

W.Z. and L.X. designed, performed experiments and wrote original draft; G.J. and Y.G. performed experiments and wrote original draft; J.S. performed experiments and revised the manuscript; Y.M., G.W., J.F. W.L. and S.Z. performed experiments and analyzed the data; Y.Y. and X.Y. designed experiments and revised the manuscript. All authors read and approved the final manuscript.

Funding

This work was supported by the Fundamental Research Funds for the Central Universities (2024-JYB-JBZD-065), the National Natural Science Foundation of China (No. 81973882, No. 81804119), and the Central High-Level Clinical Research Fund for Traditional Chinese Medicine Hospitals (DZMG-QNGG0010).

Data availability

The supporting raw data is available upon request from the corresponding author by email. The data was not saved by any of the qualified researchers.

Declarations

Ethics approval and consent to participate

The study was approved by the Animal Ethics Committee of Beijing University of Chinese Medicine (Approval Number: BUCM – 2023052602–2135, Beijing, China). The experimental protocol was performed according to the Guide for the Care and Use of Laboratory Animals from the National Institutes of Health (NIH Publications No. 8023).

Consent for publication

Not applicable.

Competing interests

There are no conflicts of interest to disclose.

Author details

[1]Department of Orthopedics, Dongzhimen Hospital, Beijing University of Chinese Medicine, Beijing 100700, PR China
[2]School of Traditional Chinese Medicine, Beijing University of Chinese Medicine, Beijing 100029, China

Received: 25 October 2024 / Accepted: 3 March 2025
Published online: 24 March 2025

References

1. Skinnider MA, Gautier M, Teo AYY, et al. Single-cell and Spatial atlases of spinal cord injury in the tabulae paralytica. Nature. 2024;631(8019):150–63.
2. Moritz C, Field-Fote EC, Tefertiller C, et al. Non-invasive spinal cord electrical stimulation for arm and hand function in chronic tetraplegia: a safety and efficacy trial. Nat Med. 2024;30(5):1276–83.
3. Kumar R, Lim J, Mekary RA, et al. Traumatic spinal injury: global epidemiology and worldwide volume. World Neurosurg. 2018;113:e345–63.
4. Xu L, Zhong W, Liu C, et al. Timing of decompression in central cord syndrome: a systematic review and meta-analysis. Eur Spine J. 2024;33(9):3593–601.
5. Tian T, Zhang S, Yang M. Recent progress and challenges in the treatment of spinal cord injury. Protein Cell. 2023;14(9):635–52.
6. Zheng B, Tuszynski MH. Regulation of axonal regeneration after mammalian spinal cord injury. Nat Rev Mol Cell Biol. 2023;24(6):396–413.
7. Hu X, Xu W, Ren Y, et al. Spinal cord injury: molecular mechanisms and therapeutic interventions. Signal Transduct Target Ther. 2023;8(1):245.
8. Li J, Luo W, Xiao C, et al. Recent advances in endogenous neural stem/progenitor cell manipulation for spinal cord injury repair. Theranostics. 2023;13(12):3966–87.
9. Bang WS, Han I, Mun SA, et al. Electrical stimulation promotes functional recovery after spinal cord injury by activating endogenous spinal cord-derived neural stem/progenitor cell: an in vitro and in vivo study. Spine J. 2024;24(3):534–53.
10. Deng Q, Ma L, Yang Y, et al. Effect of electroacupuncture stimulation on proliferation and differentiation of endogenous neural stem cells in rats with spinal cord injury. Mol Neurobiol. 2024;61(2):635–45.
11. Sherawat K, Mehan S. Tanshinone-IIA mediated neuroprotection by modulating neuronal pathways. Naunyn Schmiedebergs Arch Pharmacol. 2023;396(8):1647–67.
12. Subedi L, Gaire BP, Tanshinone IIA. A phytochemical as a promising drug candidate for neurodegenerative diseases. Pharmacol Res. 2021;169:105661.
13. Zhou ZY, Zhao WR, Zhang J, et al. Sodium Tanshinone IIA sulfonate: A review of Pharmacological activity and pharmacokinetics. Biomed Pharmacother. 2019;118:109362.
14. Song YQ, Lin WJ, Hu HJ, et al. Sodium Tanshinone IIA sulfonate attenuates sepsis-associated brain injury via inhibiting NOD-like receptor 3/caspase-1/gasdermin D-mediated pyroptosis. Int Immunopharmacol. 2023;118:110111.
15. Luo D, Li X, Hou Y, et al. Sodium Tanshinone IIA sulfonate promotes spinal cord injury repair by inhibiting blood spinal cord barrier disruption in vitro and in vivo. Drug Dev Res. 2022;83(3):669–79.
16. Zeng J, Gao WW, Yang H, et al. Sodium Tanshinone IIA sulfonate suppresses microglia polarization and neuroinflammation possibly via regulating miR-125b-5p/STAT3 axis to ameliorate neuropathic pain. Eur J Pharmacol. 2024;972:176523.
17. Yang YD, Yu X, Wang XM, et al. Tanshinone IIA improves functional recovery in spinal cord injury-induced lower urinary tract dysfunction. Neural Regen Res. 2017;12(2):267–75.
18. Basso DM, Beattie MS, Bresnahan JC. A sensitive and reliable locomotor rating scale for open field testing in rats. J Neurotrauma. 1995;12(1):1–21.
19. Rivlin AS, Tator CH. Objective clinical assessment of motor function after experimental spinal cord injury in the rat. J Neurosurg. 1977;47(4):577–81.
20. Platta CS, Greenblatt DY, Kunnimalaiyaan M, et al. Valproic acid induces Notch1 signaling in small cell lung cancer cells. J Surg Res. 2008;148(1):31–7.
21. Zipser CM, Cragg JJ, Guest JD, et al. Cell-based and stem-cell-based treatments for spinal cord injury: evidence from clinical trials. Lancet Neurol. 2022;21(7):659–70.
22. Ma D, Fu C, Li F, et al. Functional biomaterials for modulating the dysfunctional pathological microenvironment of spinal cord injury. Bioact Mater. 2024;39:521–43.
23. Xu L, Yang Y, Zhong W, et al. Comparative efficacy of five most common traditional Chinese medicine monomers for promoting recovery of motor function in rats with blunt spinal cord injury: a network meta-analysis. Front Neurol. 2023;14:1165076.
24. Liu Q, Zhou S, Wang X, et al. Apelin alleviated neuroinflammation and promoted endogenous neural stem cell proliferation and differentiation after spinal cord injury in rats. J Neuroinflammation. 2022;19(1):160.
25. Zhang J, Shang J, Ding H et al. Nicotinamide riboside promotes the proliferation of endogenous neural stem cells to repair spinal cord injury. Stem Cell Rev Rep. 2024 Jun 28.
26. Hosseini SM, Borys B, Karimi-Abdolrezaee S. Neural stem cell therapies for spinal cord injury repair: an update on recent preclinical and clinical advances. Brain. 2024;147(3):766–93.
27. Gilbert EAB, Lakshman N, Lau KSK, et al. Regulating endogenous neural stem cell activation to promote spinal cord injury repair. Cells. 2022;11(5):846.
28. Stenudd M, Sabelström H, Frisén J. Role of endogenous neural stem cells in spinal cord injury and repair. JAMA Neurol. 2015;72(2):235–7.
29. Liu S, Chen Z. Employing endogenous NSCs to promote recovery of spinal cord injury. Stem Cells Int. 2019;2019:1958631.
30. Jin Y, Song Y, Lin J, et al. Role of inflammation in neurological damage and regeneration following spinal cord injury and its therapeutic implications. Burns Trauma. 2023;11:tkac054.
31. Hellenbrand DJ, Quinn CM, Piper ZJ, et al. Inflammation after spinal cord injury: a review of the critical timeline of signaling cues and cellular infiltration. J Neuroinflammation. 2021;18(1):284.
32. Grégoire CA, Goldenstein BL, Floriddia EM, et al. Endogenous neural stem cell responses to stroke and spinal cord injury. Glia. 2015;63(8):1469–82.
33. Liu D, Shen H, Zhang K, et al. Functional hydrogel Co-Remolding migration and differentiation microenvironment for severe spinal cord injury repair. Adv Healthc Mater. 2024;13(3):e2301662.
34. Liu S, Liu B, Li Q, et al. Transplantation of fibrin-thrombin encapsulated human induced neural stem cells promotes functional recovery of spinal cord injury rats through modulation of the microenvironment. Neural Regen Res. 2024;19(2):440–6.
35. Wu C, Ji C, Qian D et al. Contribution of ApoB-100/SORT1-Mediated immune microenvironment in regulating oxidative stress, inflammation, and ferroptosis after spinal cord injury. Mol Neurobiol. 2024 Feb 10.
36. Wang J, Ye Z, Zheng S, et al. Lingo-1 ShRNA and Notch signaling inhibitor DAPT promote differentiation of neural stem/progenitor cells into neurons. Brain Res. 2016;1634:34–44.
37. Feng X, Zhang G, Feng D, et al. Spinal cord extracts from injured spinal cord impede differentiation of rat embryonic neural stem cells into neurons through regulating Notch signaling pathway. Int J Clin Exp Pathol. 2019;12(10):3855–61.
38. Luan Y, Zhang H, Ma K, et al. CCN3/NOV regulates proliferation and neuronal differentiation in mouse hippocampal neural stem cells via the activation of the Notch/PTEN/AKT pathway. Int J Mol Sci. 2023;24(12):10324.
39. Dias TB, Yang YJ, Ogai K, et al. Notch signaling controls generation of motor neurons in the lesioned spinal cord of adult zebrafish. J Neurosci. 2012;32(9):3245–52.
40. Zhong L, Wang J, Wang P, et al. Neural stem cell-derived exosomes and regeneration: cell-free therapeutic strategies for traumatic brain injury. Stem Cell Res Ther. 2023;14(1):198.
41. Otsuki L, Brand AH. Quiescent neural stem cells for brain repair and regeneration: lessons from model systems. Trends Neurosci. 2020;43(4):213–26.
42. Yu J, Chen G, Zhu H, et al. Metabolic and proteostatic differences in quiescent and active neural stem cells. Neural Regen Res. 2024;19(1):43–8.
43. Wang M, Yu L, Zhu LY, et al. Cytokines induce monkey neural stem cell differentiation through Notch signaling. Biomed Res Int. 2020;2020:1308526.
44. Peng Z, Li X, Fu M, et al. Inhibition of Notch1 signaling promotes neuronal differentiation and improves functional recovery in spinal cord injury through suppressing the activation of Ras homolog family member A. J Neurochem. 2019;150(6):709–22.
45. Qian D, Li L, Rong Y, et al. Blocking Notch signal pathway suppresses the activation of neurotoxic A1 astrocytes after spinal cord injury. Cell Cycle. 2019;18(21):3010–29.

Publisher's note